QUANTITATIVE TEXTURE ANALYSIS OF BLANKET FILMS AND INTERCONNECTS

K. J. Kozaczek, D. S. Kurtz

HyperNex, Inc.

State College, PA 16801

Kozaczek@vicon.net

HypernexInc.com

Workshop on Texture in Electronic Applications

NIST, Gaithersburg, MD, October 10-11, 2000

HyperNex

Outline

1. Overview QTA: Orientation Distribution Function (ODF)
- measurement of pole figures,
- transformations from pole figures to ODF
- precision and accuracy issues
- graphical and numerical representation of texture data

2. How are texture measurements and analysis in thin film structures different from a traditional approach for bulk materials?
- experimental requirements and solutions,
- ODF analysis

3. Examples of QTA applied to copper metallization technology.

Orientation of Individual Crystallites: Definition of Euler Angles

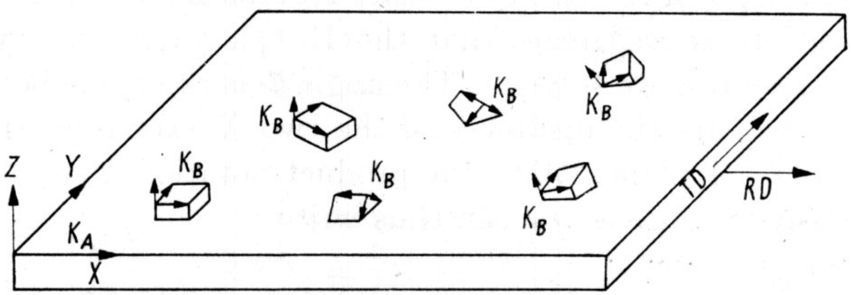

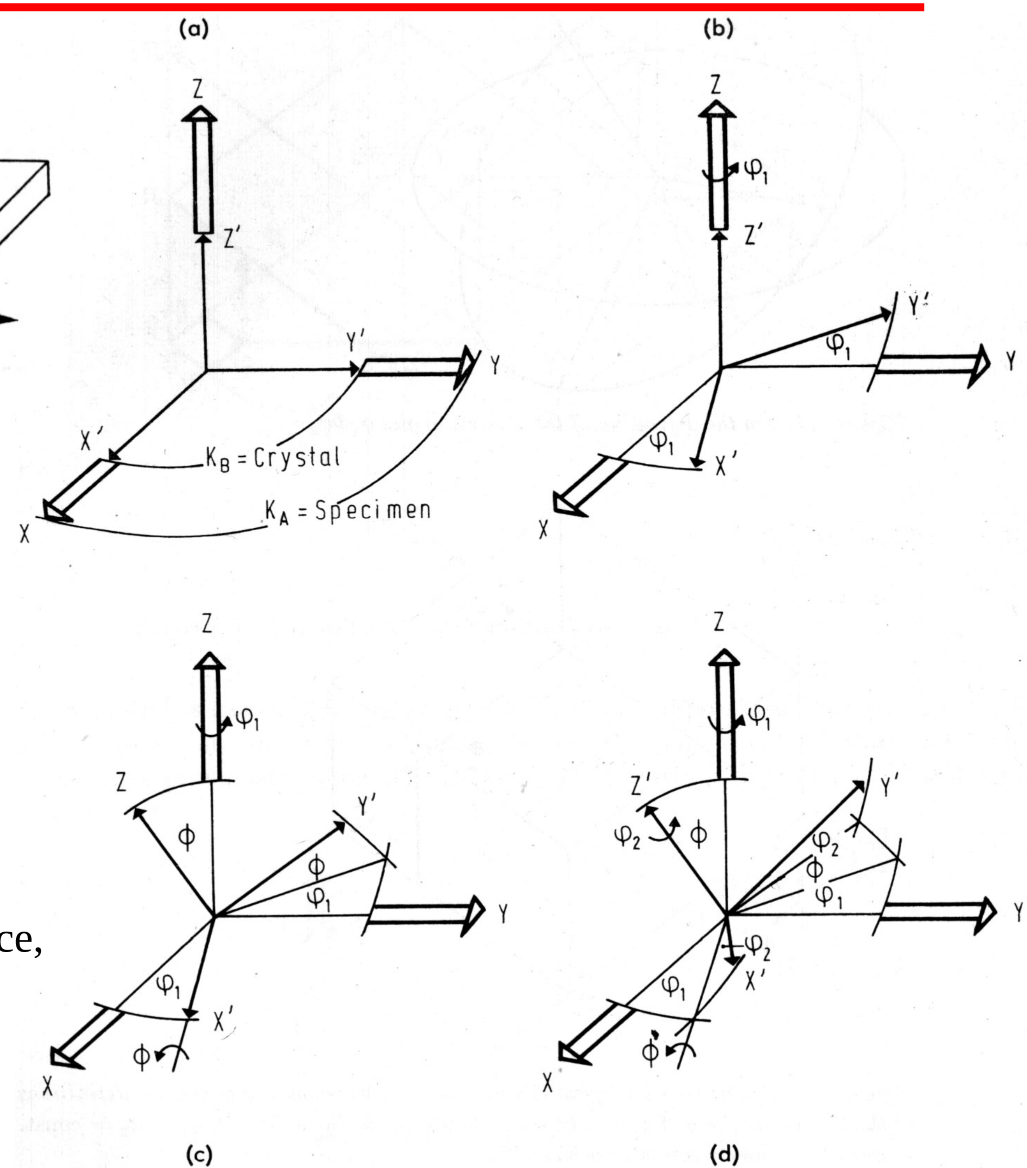

$$g : [K_A \rightarrow K_B)$$

$$g \equiv (\varphi_1, \phi, \varphi_2)$$

H.J. Bunge, Texture Analysis in Materials Science, (Butterworths, London, 1982)

Rotation *g* Defines Crystal Orientation

- ***g*** may be specified in numerous ways:
  - ***g***=[g_{ij}] orientation matrix 9 parameters
  - ***g***={υψω} axis-rotation angle 3 parameters
  - ***g***=(hkl)[uvw] metallurgical 6 parameters
  - ***g***={$\phi_1 \Phi \phi_2$} Euler angles 3 parameters
- Several variants of Euler angles are in use:
  - {$\phi_1 \Phi \phi_2$} H.-J. Bunge, Texture Analysis in Materials Science, Butterworths, London, 1982.
  - {ΨΘΦ} R. J. Roe, *J. Appl. Phys*. **36** (1965) 2024-2031.
  - {αβγ} S. Matthies, G. W. Vinel, K. Helming, Standard Distributions in Texture Analysis, Academie, Berlin, 1987.

Orientation Distribution Function f(g): Definition of Texture

Orientation distribution by volume:

$$\frac{dV}{V} = f(g)dg$$

Where: dV is the volume of crystallites that have the orientation ***g*** within the element of orientation dg, and V is the total sample volume.

Orientation distribution by number of crystallites:

$$\frac{dN}{N} = n(g)dg$$

$$dg = \frac{1}{8\pi^2}\sin\Phi d\varphi_1 d\Phi d\varphi_2$$

Experimental Methods of Texture Measurement

- Individual orientation measurement: $\boldsymbol{g}_i$ and corresponding V_i of all crystallites in the sample, construction of n(g) or f(g).
- Pole figure measurement: direct measurement of dN or dV of crystallites with two angular parameters fixed and the third varied trough all possible values, calculation of ODF from several pole figures.
- Indirect calculation of ODF from measurement of anisotropy of physical properties (elastic, magnetic, electrical).

Pole Figure Measurements by Diffraction Methods

Fixed diffraction vector method

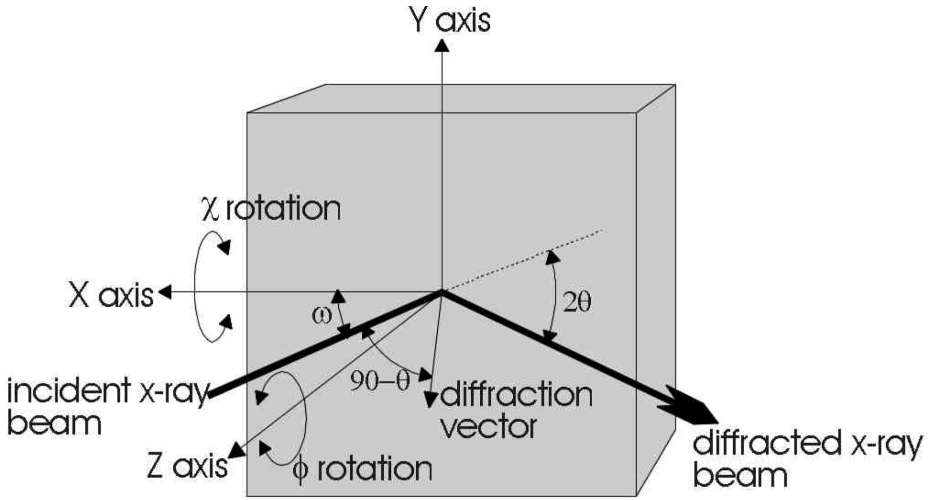

Need at least two independent rotations (e.g. Φ and χ)
but usually texture goniometers allow three sample rotations (Φ, ω and χ)

Variable diffraction vector method

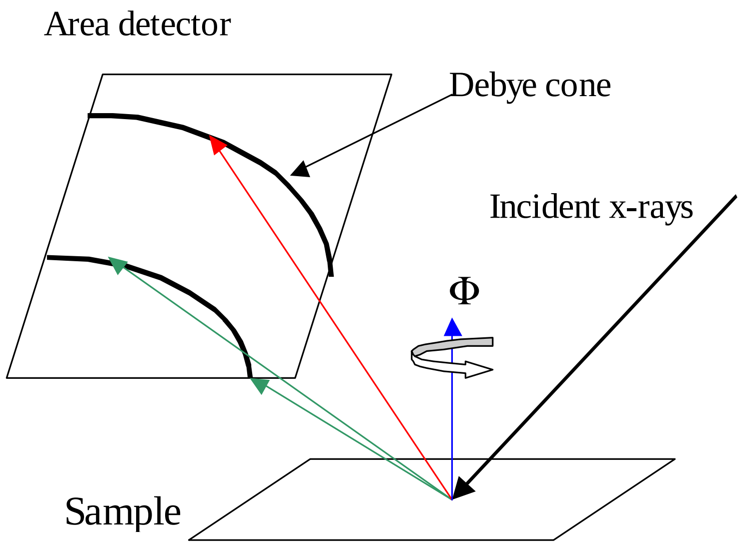

Diffraction vector varies along Debye ring and for different Debye rings

Only one sample rotation angle is needed (Φ)

Intensity Distributions Are Not Pole Figures

- **Intensity to pole density conversions include:**
  - Absorption corrections (necessary for tilts >70 degrees)
  - Defocusing corrections
  - Background corrections
  - Variable diffracting volume (especially for thin films)
- **Corrections in pole figure space:**
  - Sample misalignment
  - Parallax errors (detector space)
  - Interpolation in pole figure space
  - Pole figure normalization
- **Goniometer misalignment errors are generally not correctable (e.g. peak shifts with tilt, etc.)**
- **Individual pole figures and sets of pole figures must be self-consistent**

Asymmetric Diffraction Geometry Results in Non-Equidistant Mapping in Pole Figure Space

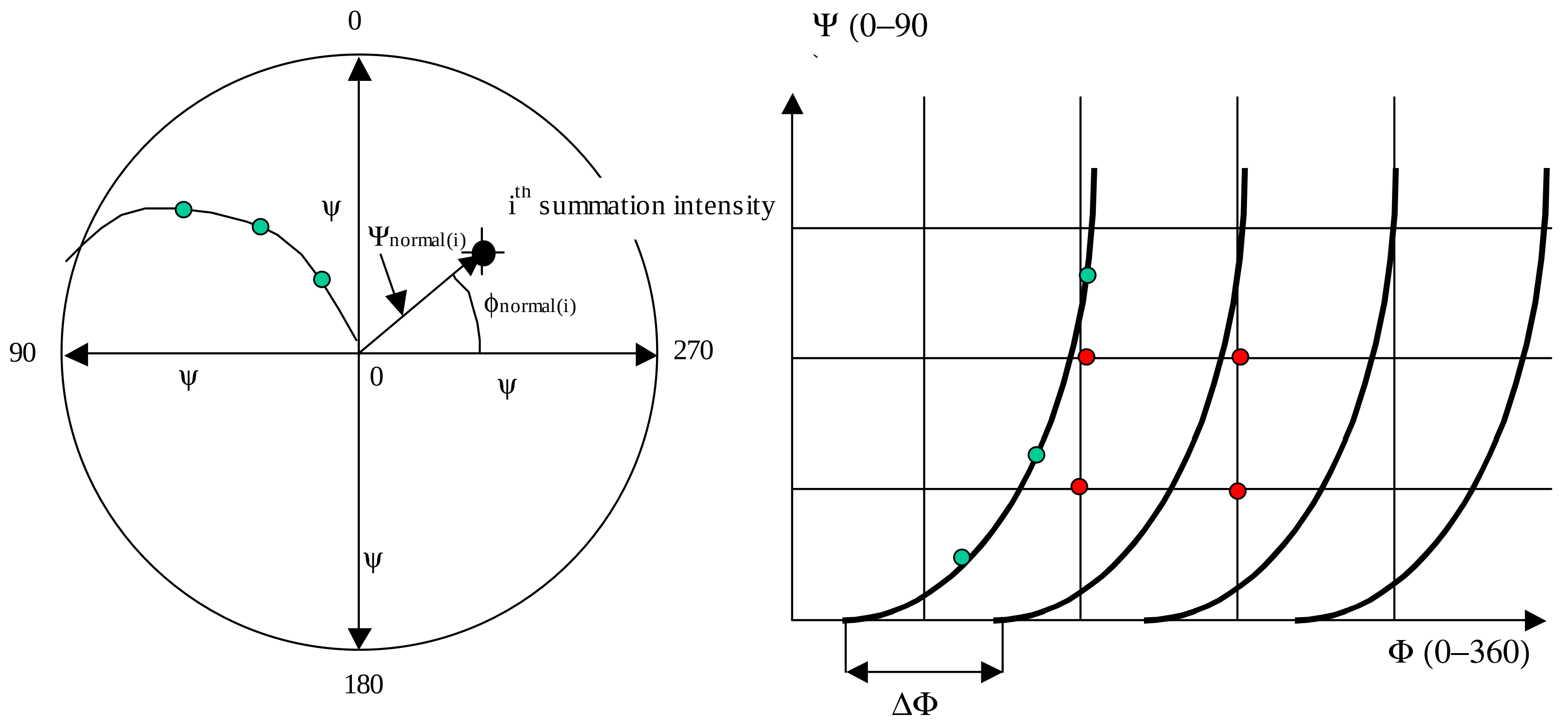

All ODF programs accept pole figure data on a equidistant mesh

Interpolation in PF space is necessary

Angular resolution of PF's must match the sharpness of measured texture

Thin Films: Experimental Specifics

- Finite thickness often requires grazing incident geometry (asymmetric diffraction)
- Tilt dependent (varying) penetration depth may hinder analysis but can be controlled
- Multilayers require additional absorption correction
- Diffracting volume changes with tilt
- Experiments always result in incomplete pole figures

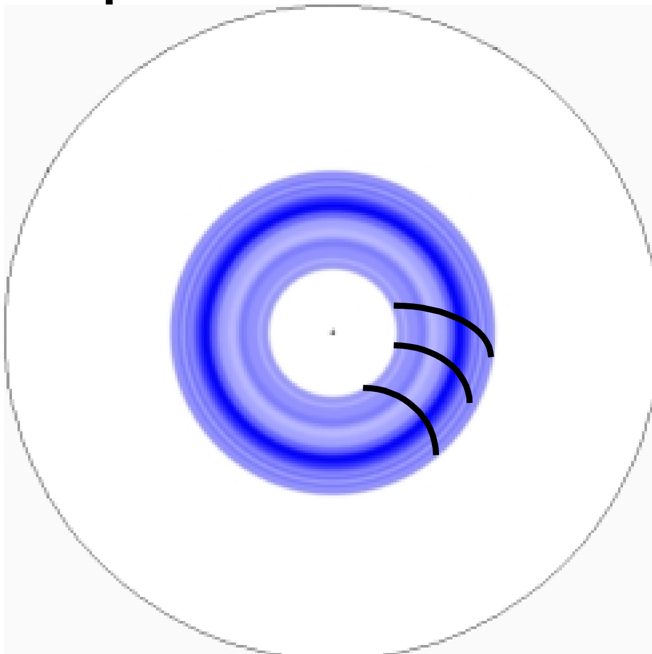

HyperNex

Pole Figure Inversion Methods

Method	Source Codes	Resolution	Solution (texture dependent)	Computer Time
Fourier Methods				
Classical harmonic	Many available; e.g., Jura et al., 1976	Limited by L	$\tilde{f}(g)$	1*
Zero range	Bunge-Esling		weak tex.: $\tilde{f}(g)$ strong tex.: $f(g)$	5
Iterative positivity	Dahms-Bunge			3
Quadratic form	Van Houtte	Residual error		10
Maximum entropy	Liang et al.		Smooth ODF	
Direct Methods				
Vector	Vadon, Schaeben	Limited by computer	weak tex.: $\tilde{f}(g)$ strong tex.: $f(g)$	10
Imhof	Imhof	Good		5
Pawlik-Pospiech	Pawlik, Pospiech			1
WIMV	Matthies-Vinel, Kallend		Smooth with strong peaks	1
Gauss correction	Lücke, Pospiech	Residual error	Strong peaks	

Wenk, Bunge, Kallend, Lucke, Matthies, Pospiech, Van Houte, ICOTOM 8, (TMS, 1988), p. 17.

Error Criteria for ODF Calculations

$$RP(\varepsilon) = \frac{1}{IJ}\sum_{i=1}^{I}\sum_{j=1}^{J}\frac{\left|PF_{ij}^{cal} - PF_{ij}^{\exp}\right|}{PF_{ij}^{\exp}}\theta(\varepsilon, PF_{ij}^{\exp})100\%$$

$$\theta(\varepsilon, x) = \{_{1}^{0}\ for_{x>\varepsilon}^{x\leq\varepsilon}$$

where: i indicates the pole figure, I is the number of pole figures taken for ODF calculation, j indicates a point on a pole figure and J is the number of points on the pole figure taken for ODF calculation

Table 2. RP error measures (practical experience, Wenk and Matthies)

RP %	Maximum deviations expected in pole figures ± m.r.d.	Applicability
0.5 - 1	0.05	Resolution of most methods
1 - 2	0.1	Excellent experimental pole figures
2 - 5	0.2	Good pole figures—weak textures
5 - 10	0.5	Good pole figures—strong textures
> 10	1.0	Problems with data

Wenk, Bunge, Kallend, Lucke, Matthies, Pospiech, Van Houte, ICOTOM 8, (TMS, 1988), p. 17.

Representations of ODF

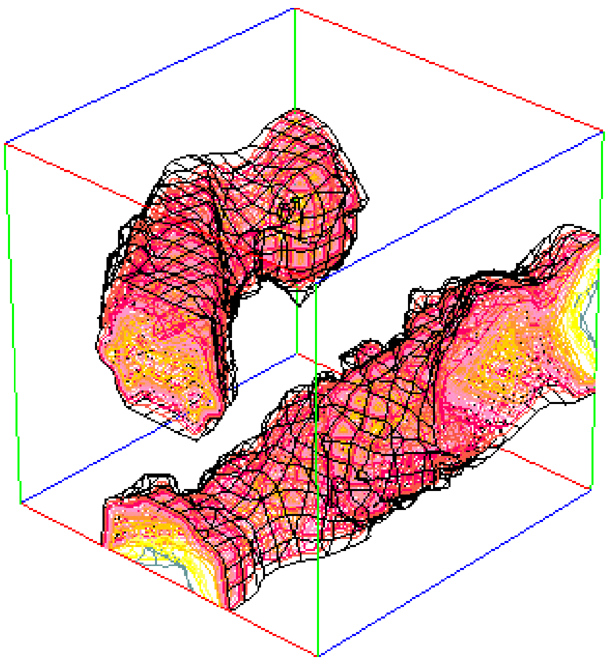

For cubic-orthorhombic symmetry ODF with 1 deg. resolution contains 729,000 values

Graphic representations are semi-quantitative and include:

-3-D cross-sections

-2-D cross-sections

-Cartesian or polar coordinates

Quantitative representation by model functions (texture components)

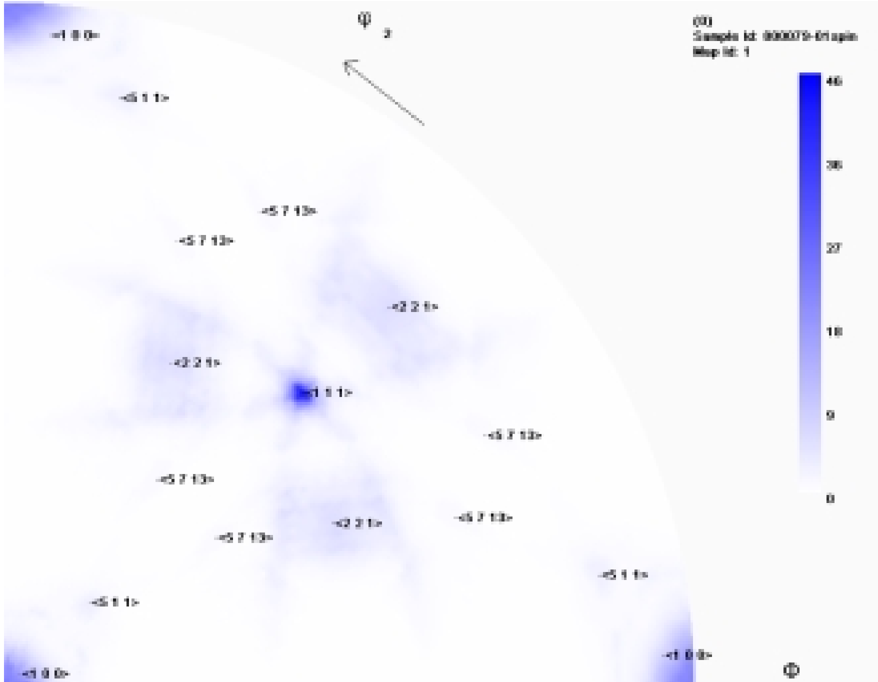

Representation of ODF by 2D and 1D Cross-Sections

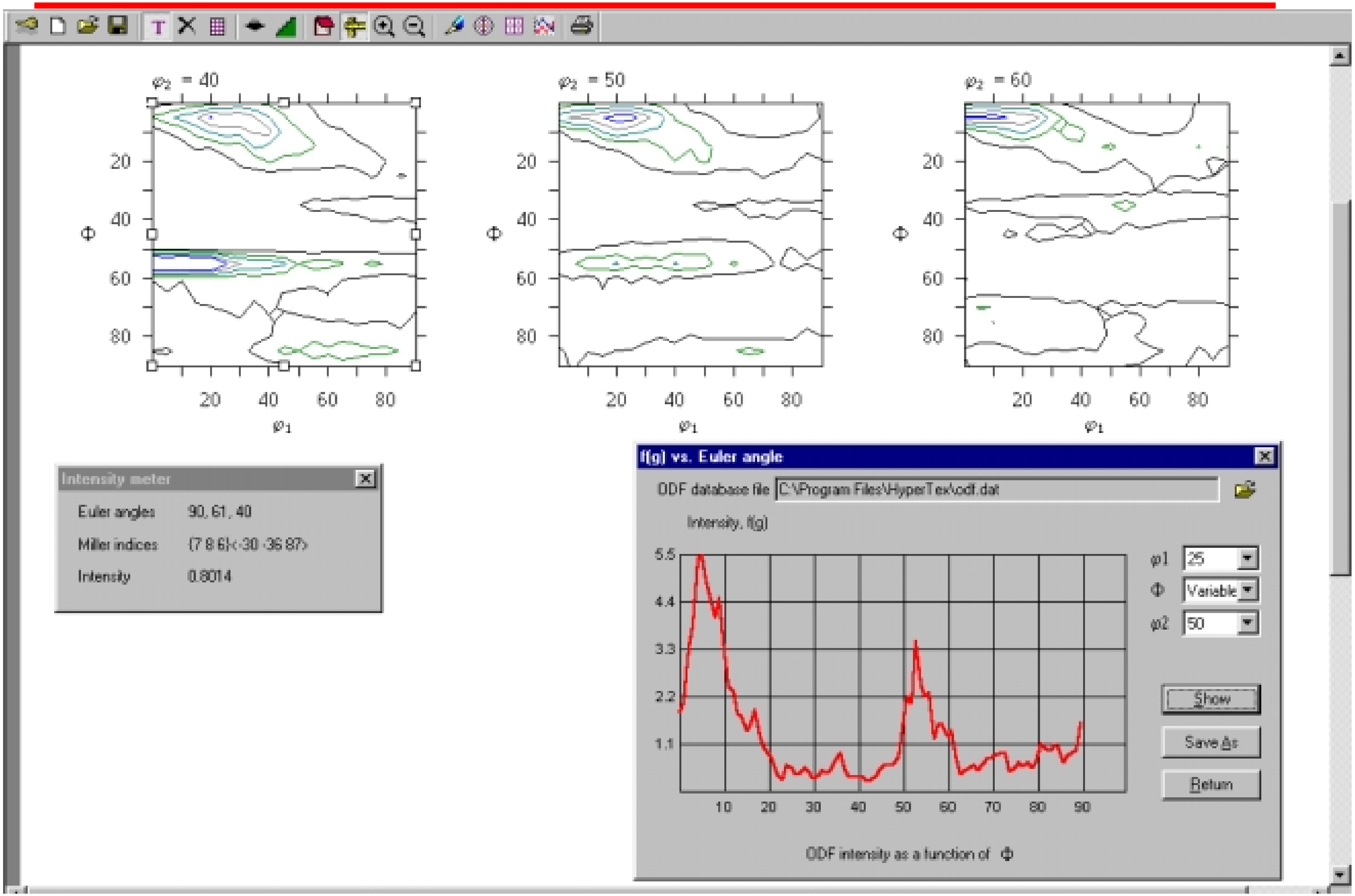

Semiconductor Industry Imposes New Requirements on Texture Analysis

- High resolution texture analysis:
  High resolution of reciprocal space mapping
  Direct methods of ODF calculations

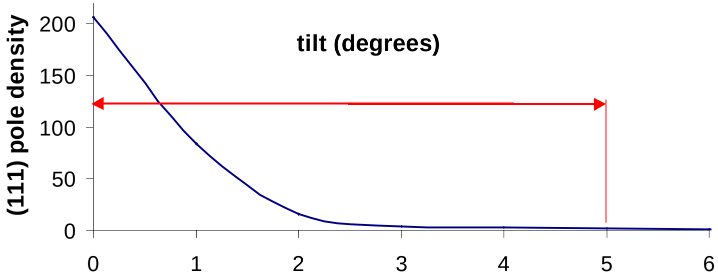

- High spatial resolution:
  Precision in beam and sample positioning
  Small x-ray beams
  Stationary sample

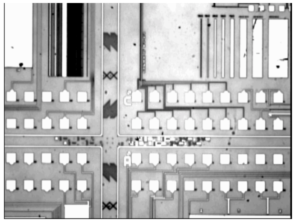

- Mapping capability
  Accommodate 200 and 300 mm wafers

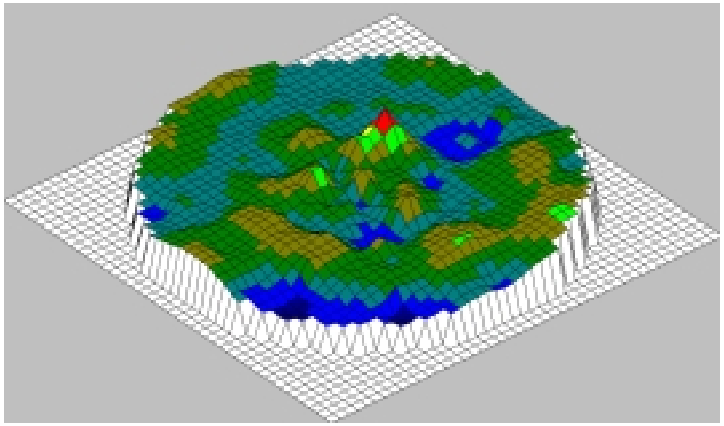

- Other: throughput, contamination control, automation

Methods Based On Series Expansion Lack Resolving Power For Sharp Textures

Effect of the expansion level l_{max} (harmonic methods) on the reproduced ODF value

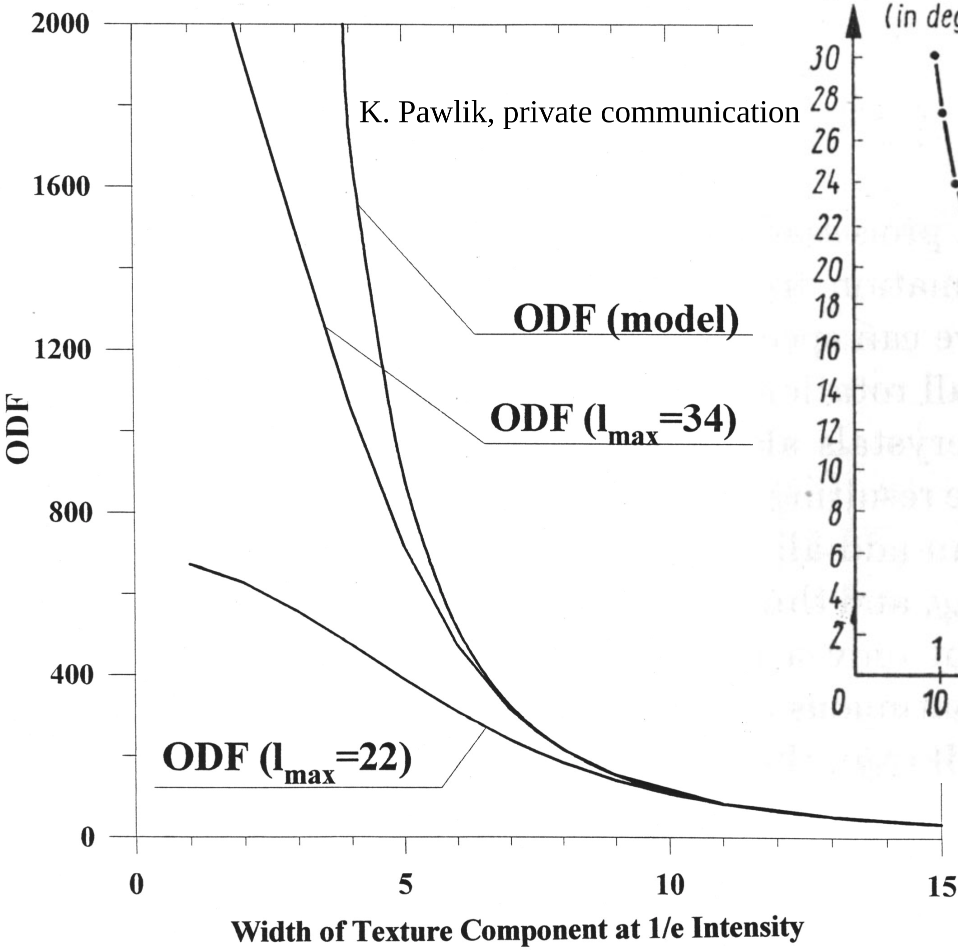

K. Pawlik, private communication

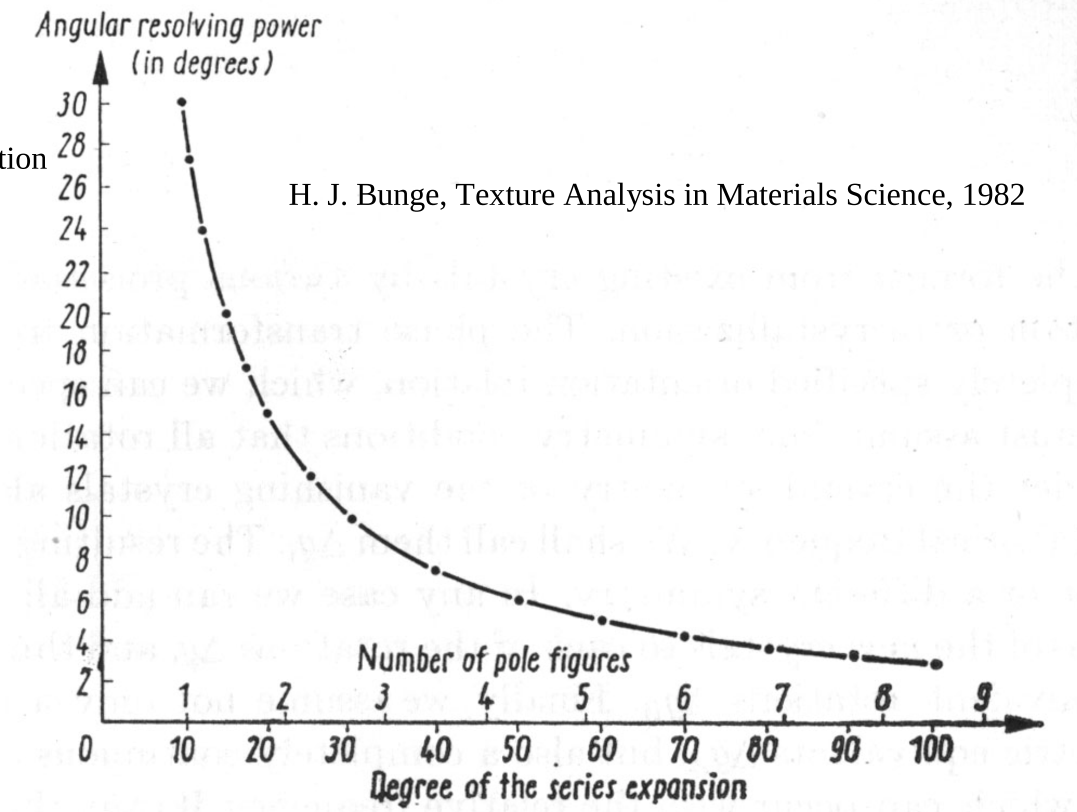

H. J. Bunge, Texture Analysis in Materials Science, 1982

Direct Methods (WIMV, ADC) With 1 Degree Resolution Are Preferred

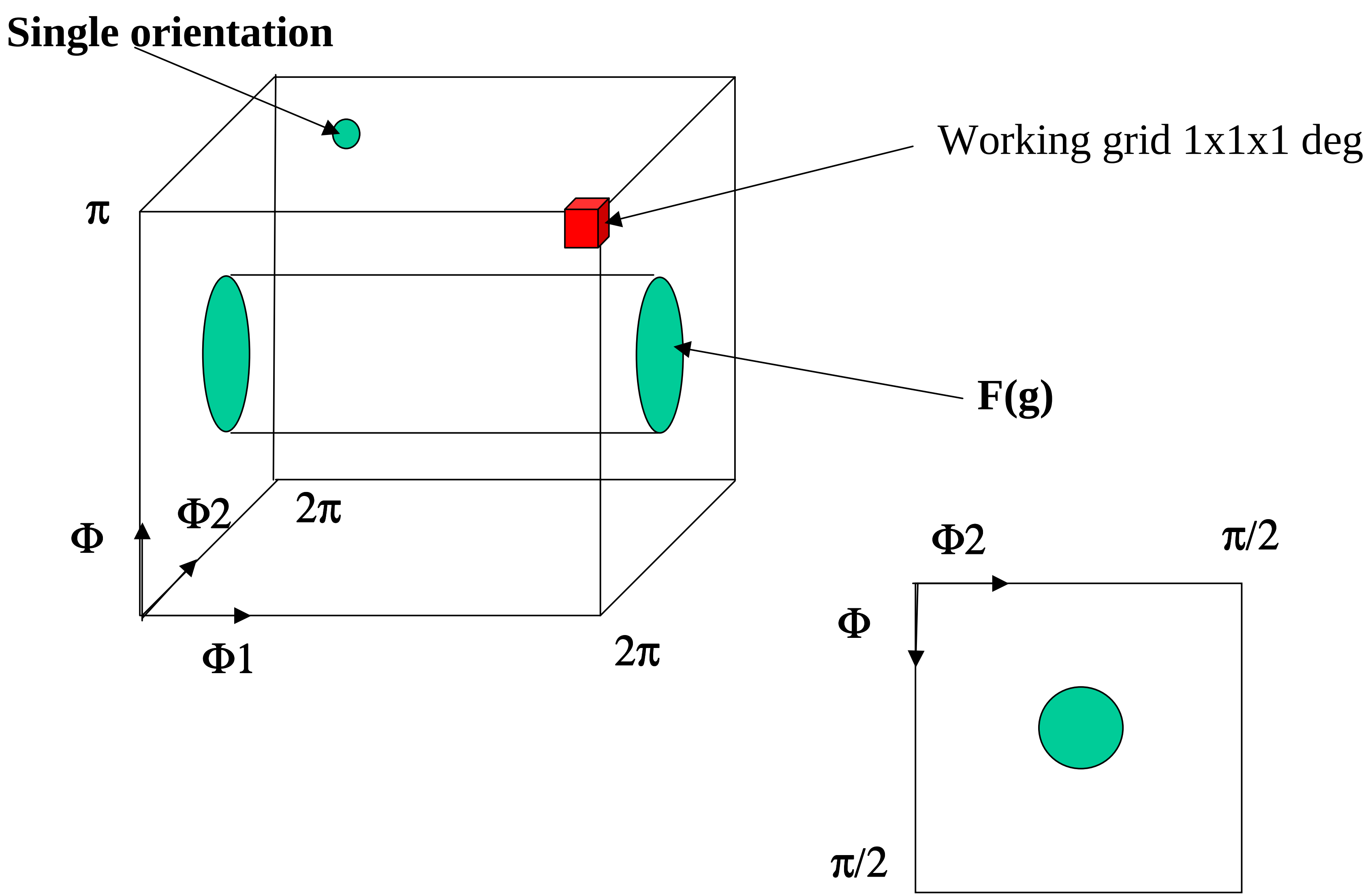

Measurement Platform of Texture Mapping Instrument

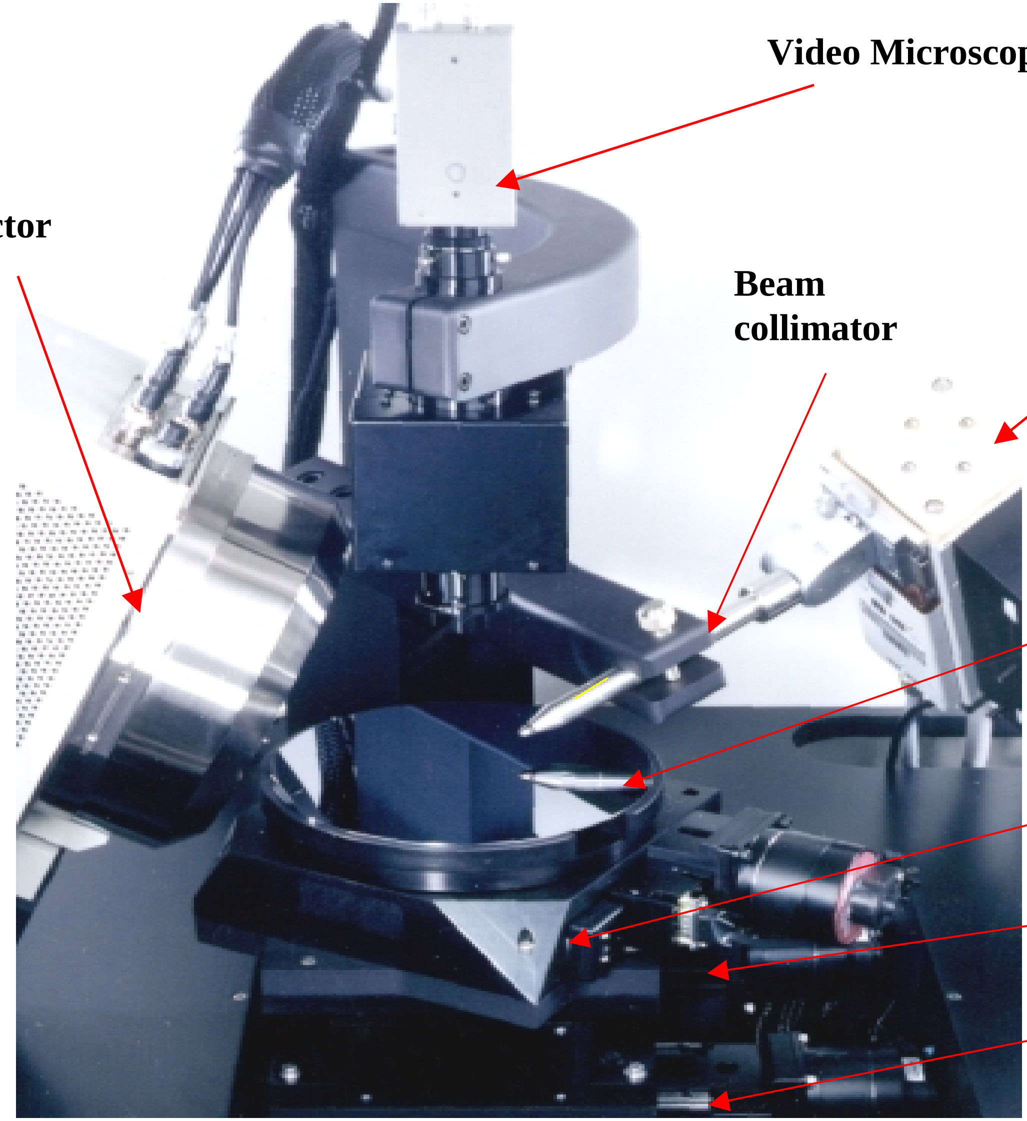

Several Incomplete Pole Figures Are Measured Simultaneously

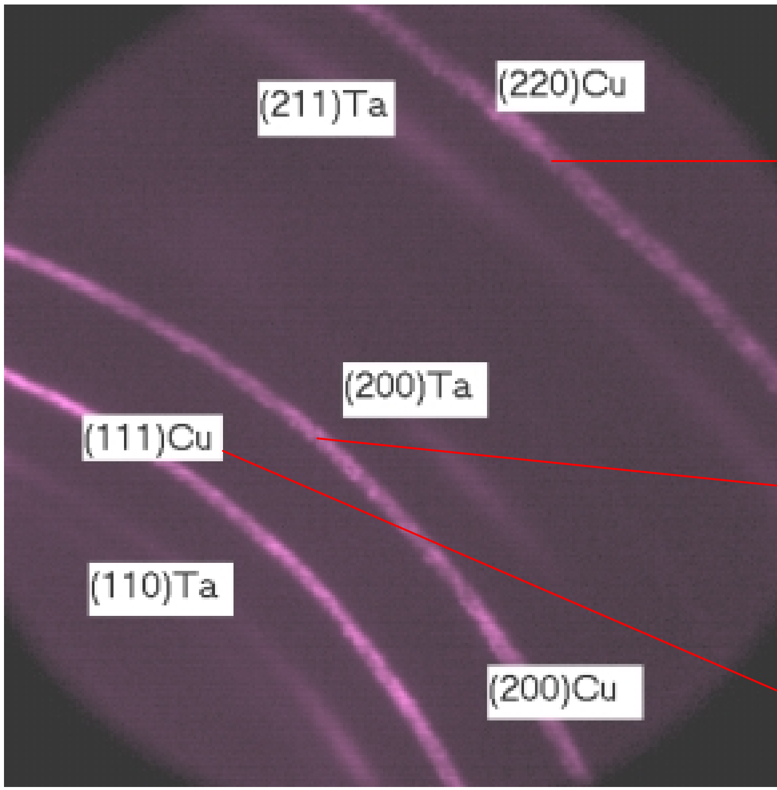

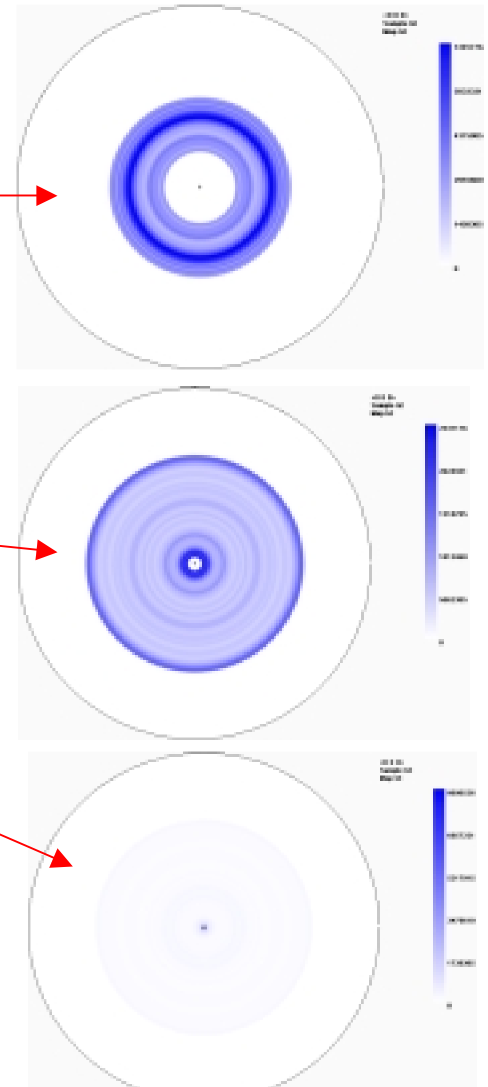

Debye rings registered on detector face

0.5 micron electroplated copper deposited on 300A thick Ta barrier layer

Pole Figure Ranges Are Optimized For Materials And Textures Typical of Semiconductor Industry

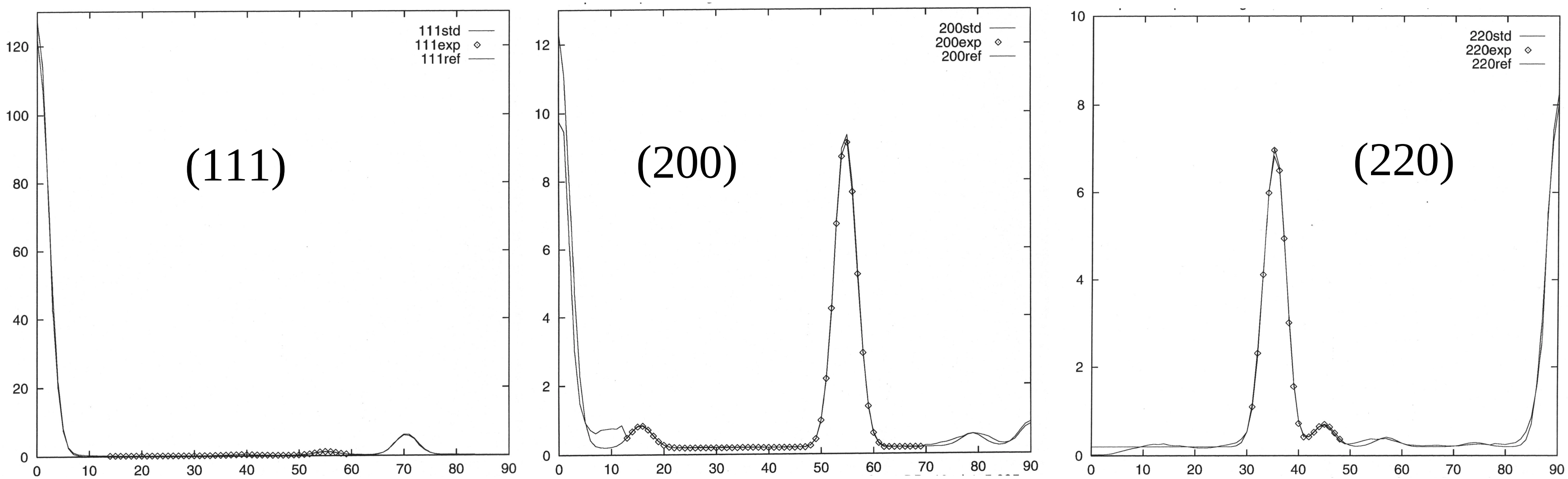

Use model functions to simulate ODF

Select ranges on PF satisfying MPDS criterion

Use partial PF to recalculate ODF

Estimate relative error (<2%)

$$RP(\varepsilon) = \frac{1}{IJ} \sum_{i=1}^{I} \sum_{j=1}^{J} \frac{| PF_{ij}^{cal} - PF_{ij}^{\text{mod}} |}{PF_{ij}^{\text{mod}}} 100\,\%$$

Quantitative Texture Analysis Offers Numerous Outputs

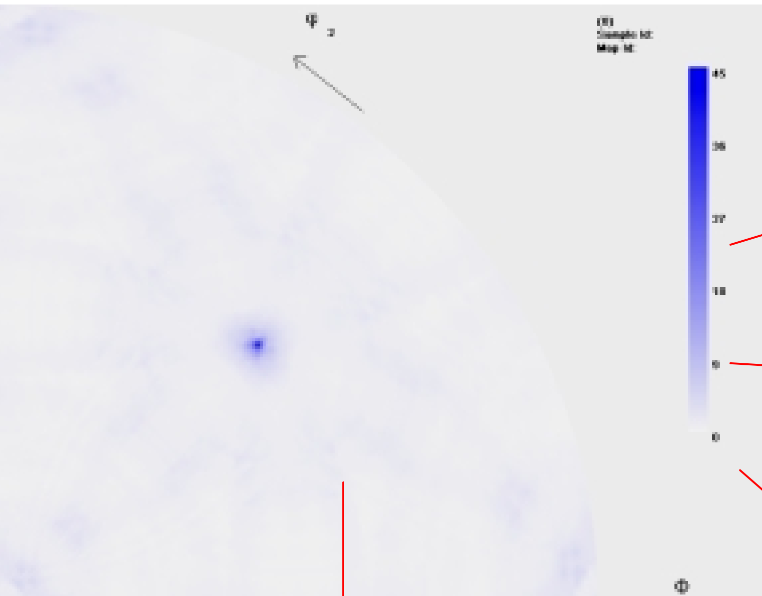

Line plots

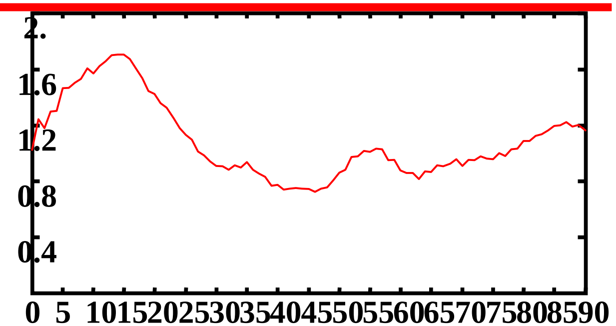

Pole figures

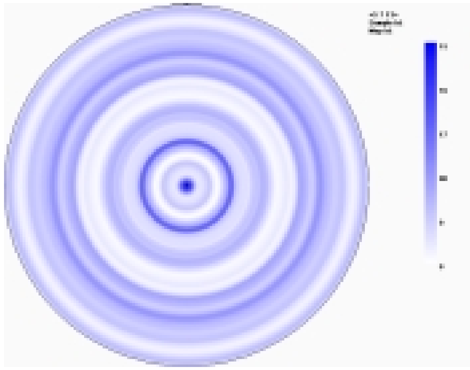

Volume fraction maps

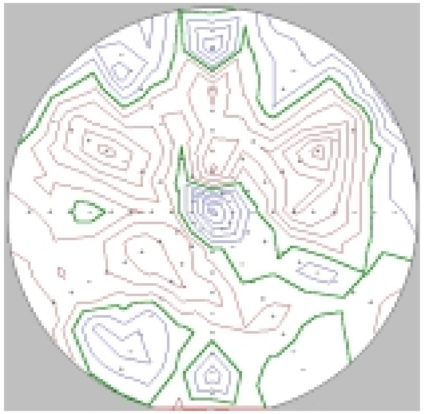

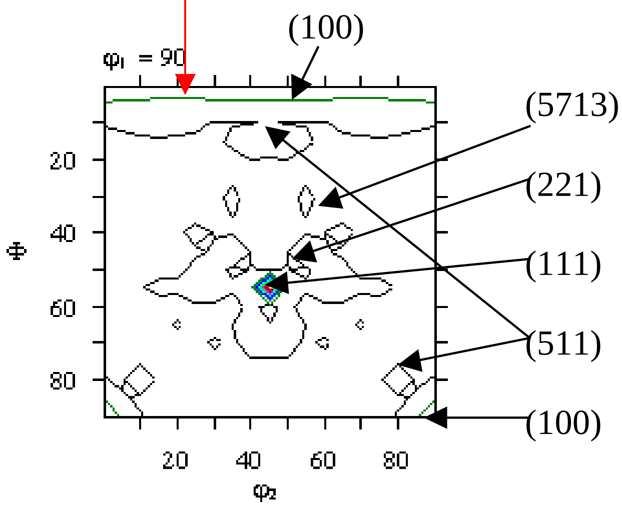

Volume Fractions of Texture Components Are A Quantitative Measure Easy to Interpret

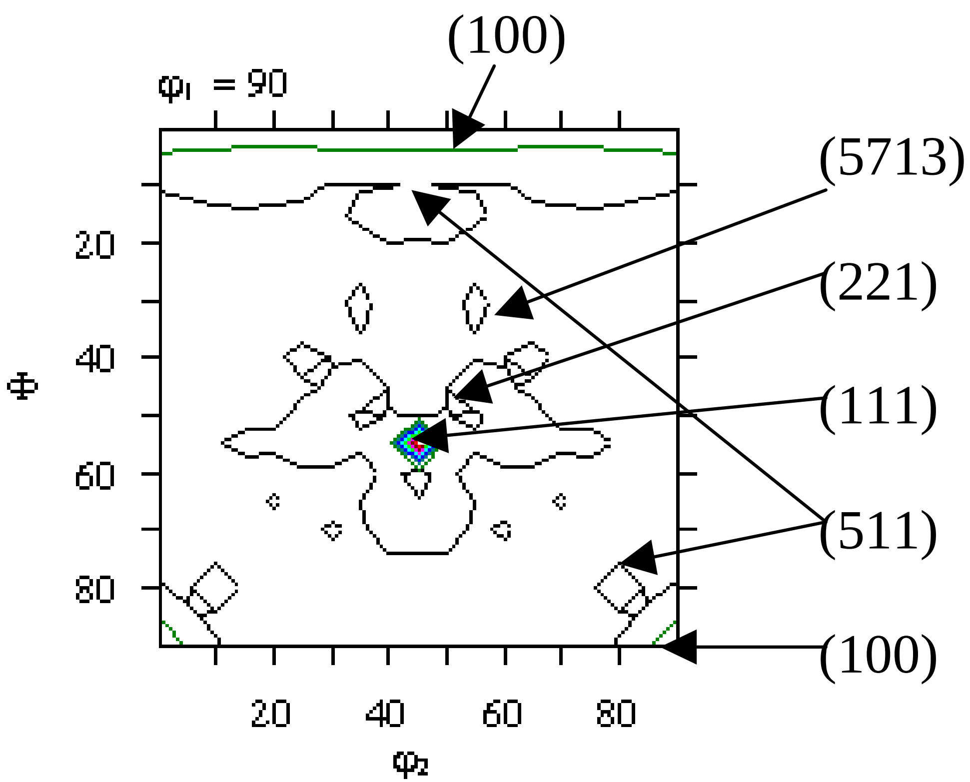

Volume fractions of texture components with cyclic fiber textures are determined with accuracy better then 5% and precision of 0.5%

$$\frac{dV}{V} = f(g)dg$$

$$dg = \frac{1}{8\pi^2} \sin \Phi d\phi 1 d\Phi d\phi 2$$

Errors in Volume Fraction Analysis Are Estimated Using Model Textures

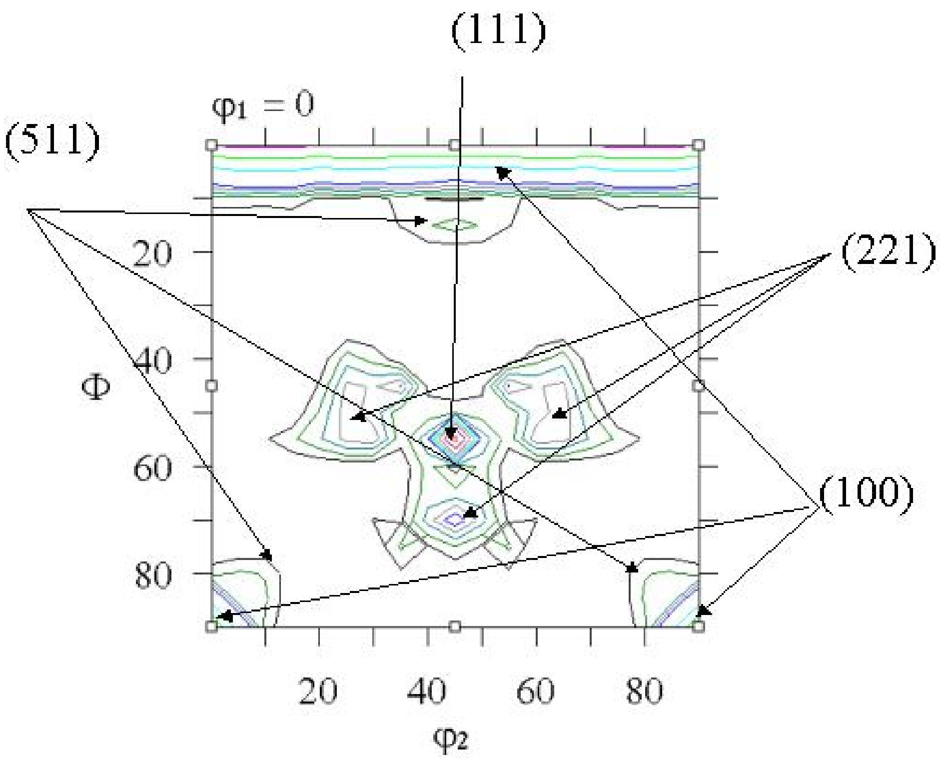

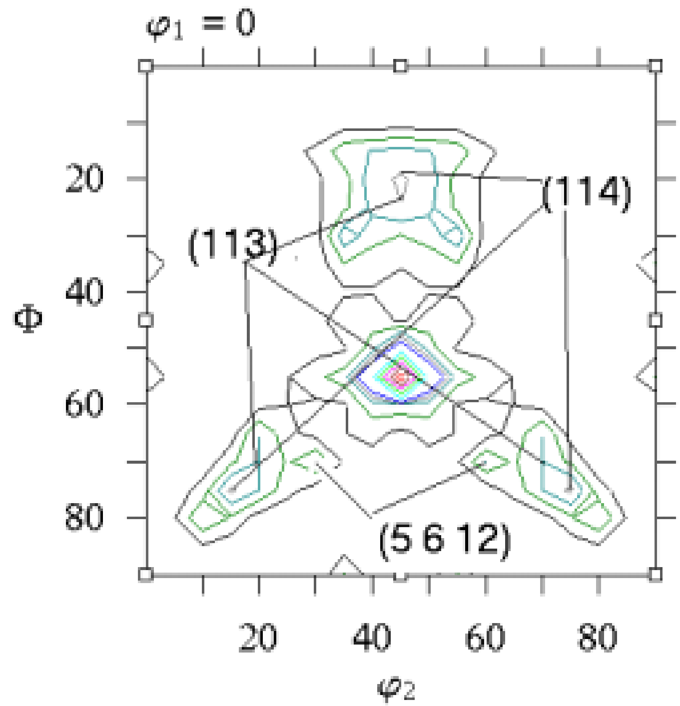

1.0µm PVD/0.25 µm EP blanket copper film annealed at 300C for 0.5 hour

1.0µm PVD/0.25 µm EP blanket copper film recrystallized at room temperature

QTA of 1.0μm PVD/0.25 μm EP blanket copper film annealed at 300C for 0.5 hour

Texture component	Volume fraction	FWHM (deg)
(111)	0.15	2.5
(511) 1-st gen. twin	0.02	3.0
(5713) 2-nd gen twin	0.01	3.0
(100)	0.25	8.0
(221) 1-st. gen. twin	0.40	9.0
Random	0.15	-

Pole Figure	RP(1) (%)	Correlation
(111)	8.9	1.00
(200)	15.1	1.00
(220)	5.0	0.98

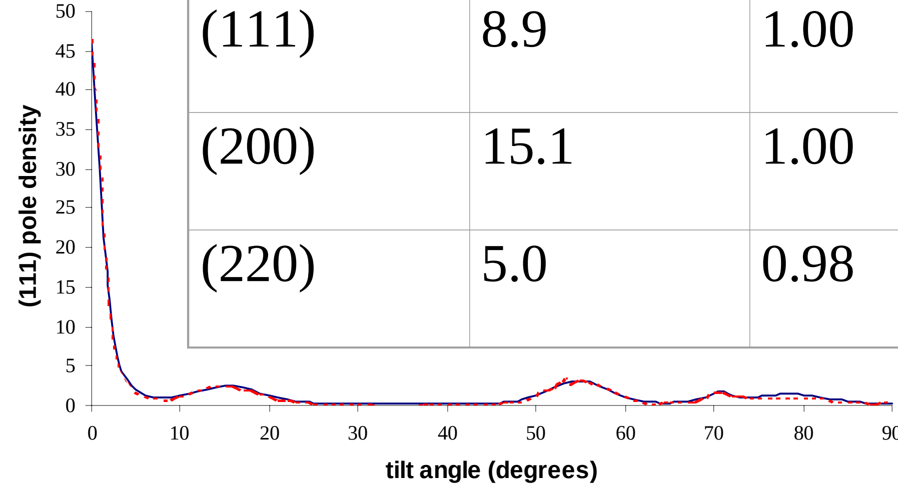

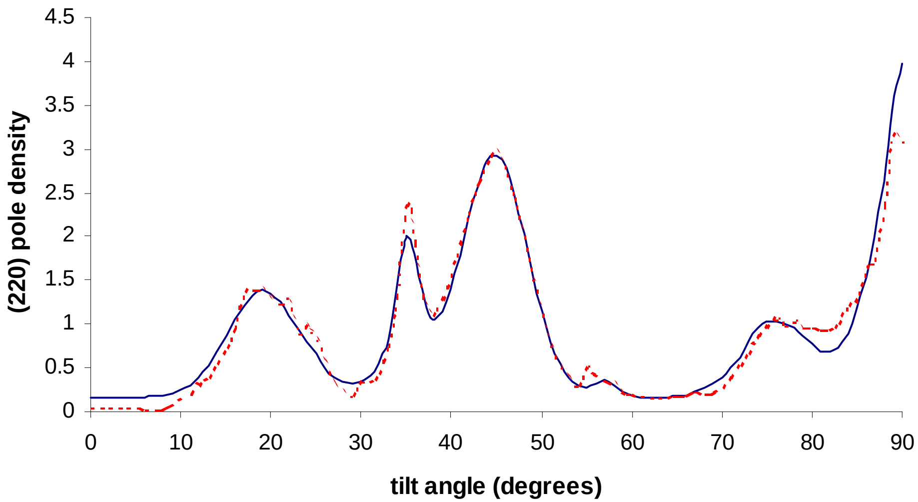

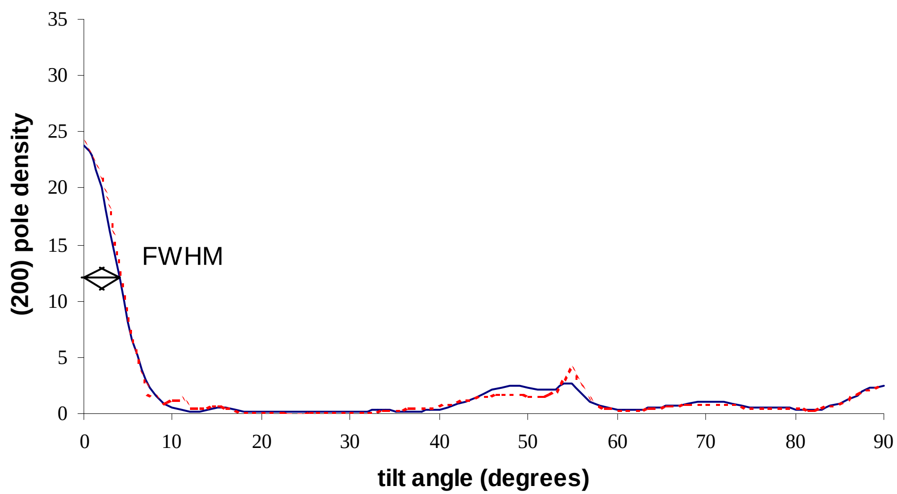

QTA for 1.0µm PVD/0.25 µm EP blanket copper film recrystallized at room temperature

(111)	0.34	4.5
(113)	0.10	7.0
(114)	0.10	8.0
(115)	0.04	4.0
(56 12)	0.15	10.0
Random	0.27	-

Pole Figure	RP(0) (%)	Correlation
(111)	9.6	0.96
(200)	9.7	0.98
(220)	14.6	0.98

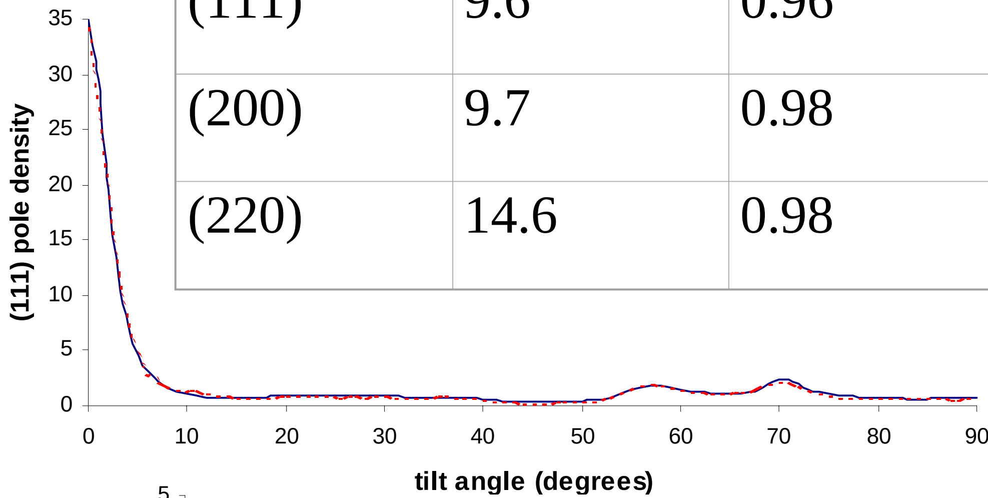

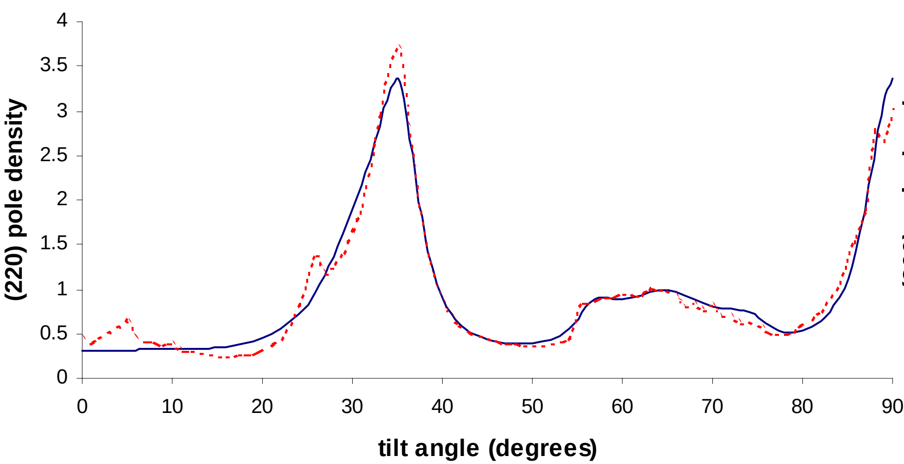

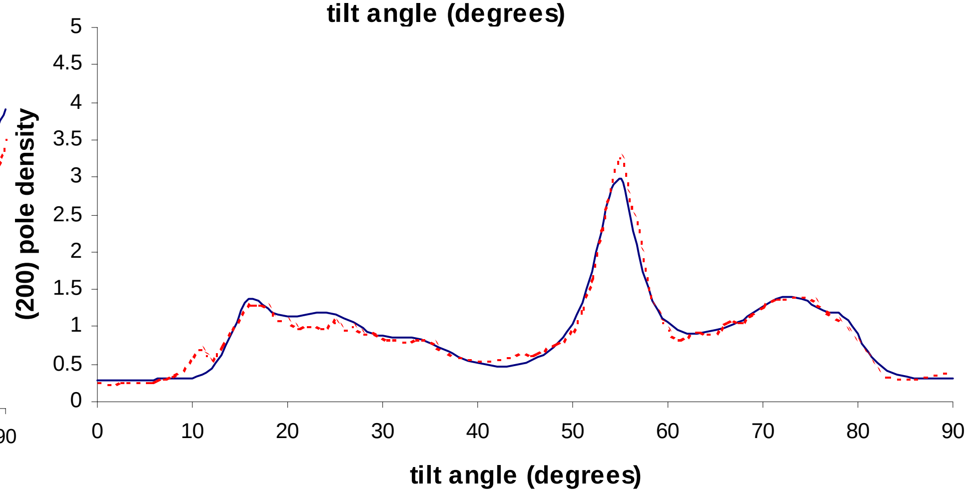

Texture Modeling Helps to Interpret Experimental Results

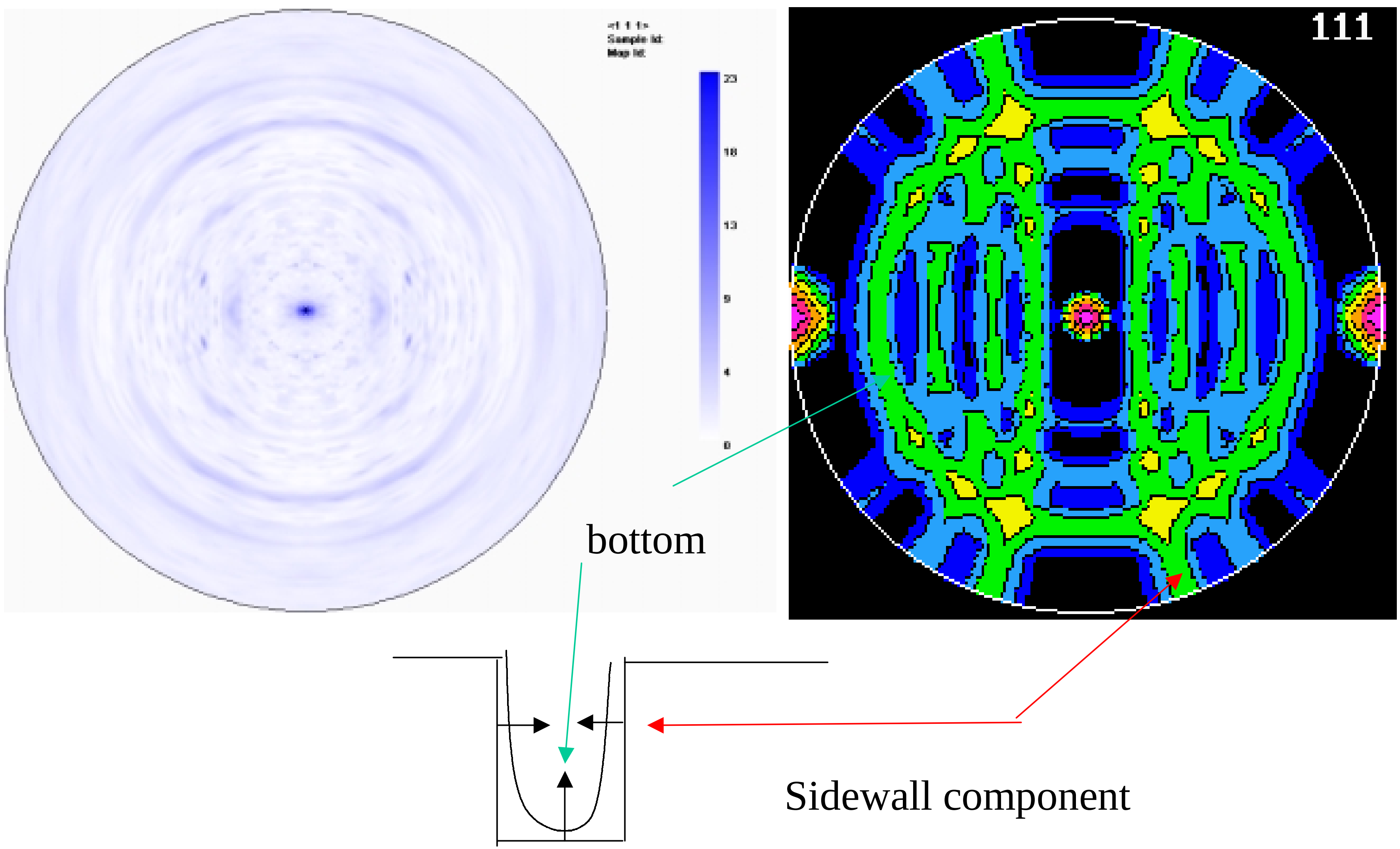

High Spatial Resolution (~100 μm) and Precision In Positioning (~10 μm) Is Often Required

Electroplated Damascene Copper +CMP,
Structure Size 300 X 500 μm^2

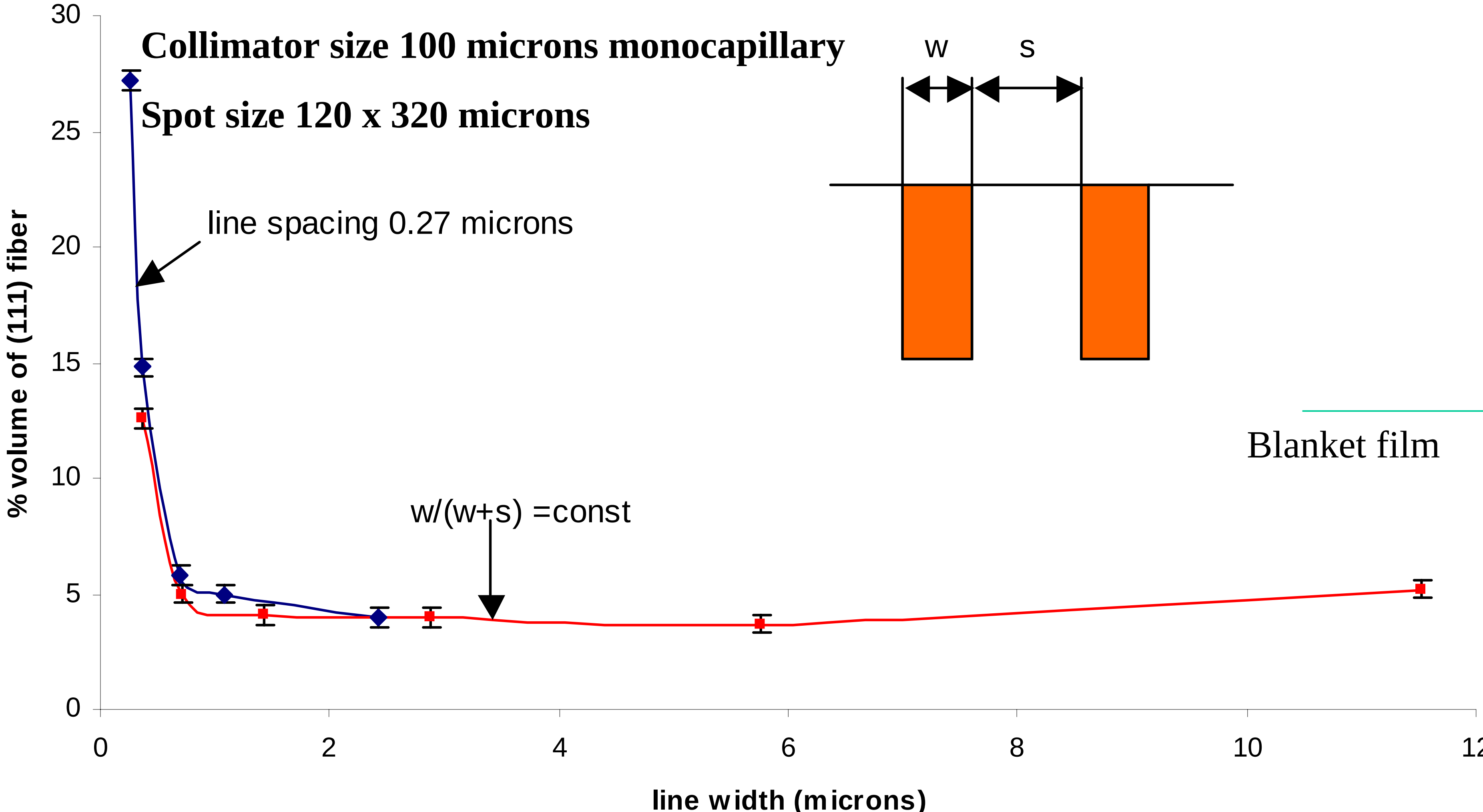

Wafer Mapping Helps to Understand Processing Variables

Distribution of volume fraction of a (111) cyclic fiber texture on a 1micron electroplated copper deposited on 200 mm wafer (30% range of variation)

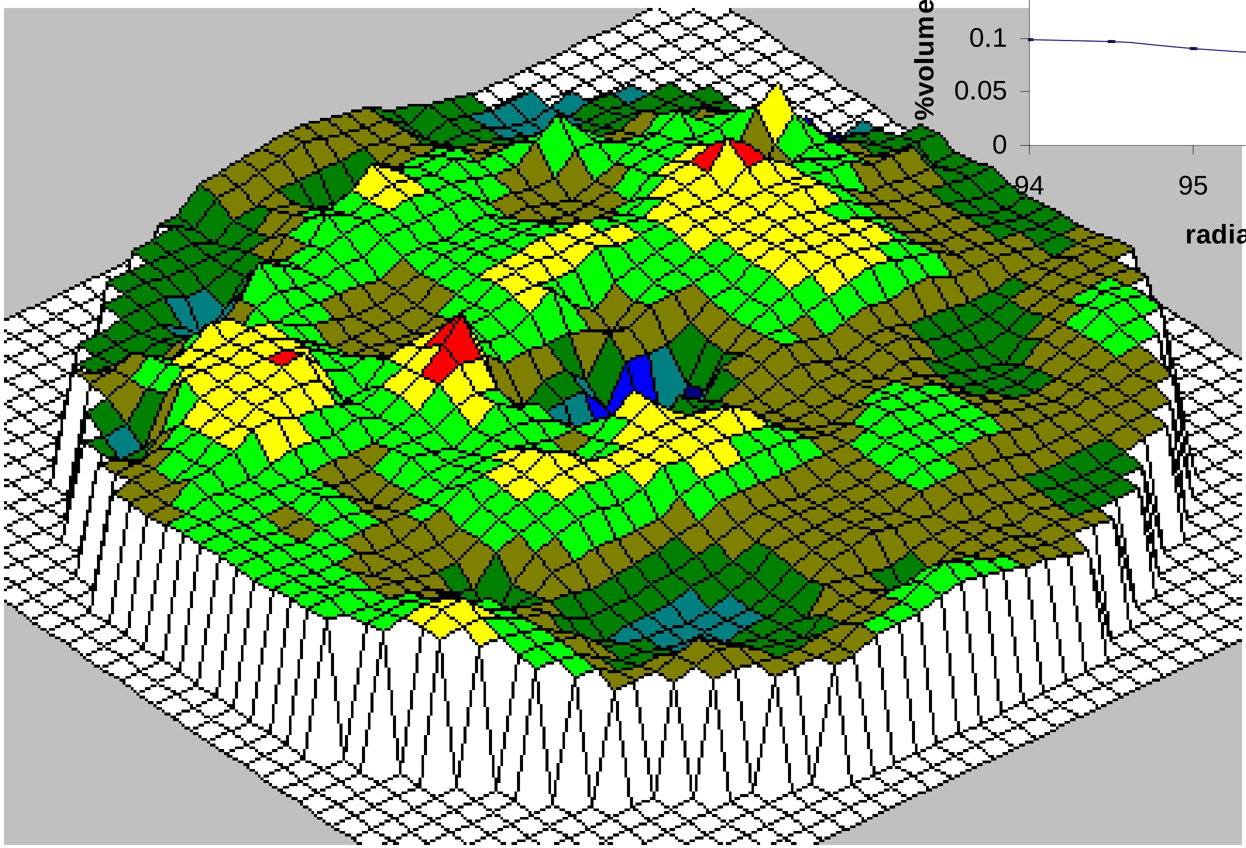

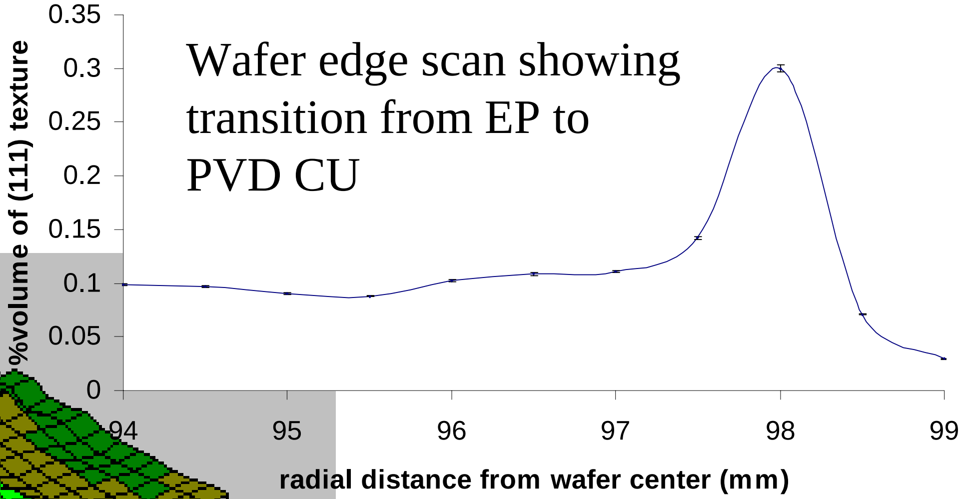

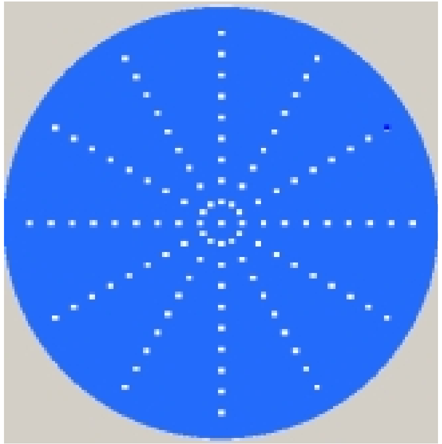

120 point map

Summary

- Quantitative texture analysis (QTA) has evolved as a powerful tool for material characterization
- In controlled circumstances QTA is operator independent and suitable for automation
- Application of QTA as a quality control tool is feasible; it has been proven in the sheet metal industry and is being evaluated in the semiconductor industry